

Sliding wear behaviour of two gamma-based titanium aluminides

A.R. Rastkar^{a,*}, A. Bloyce^b, T. Bell^a

^a School of Metallurgy and Materials, The University of Birmingham, Edgbaston, Birmingham, B15 2TT, UK

^b Balzers Limited, Tool Coating Division, Bradbourne Drive, Tilbrook, Milton Keynes, AZ MK7 8 USA

Received 10 August 1998; received in revised form 22 November 1999

Abstract

Lamellar Ti–48Al–2Nb–2Mn (at.%) and Ti–45Al–2Nb–2Mn–1B (at.%) titanium aluminides have been wear tested using a ball-on-disc configuration against a 10-mm-diameter hard steel ball under dry sliding conditions at applied loads of 3.5, 5, 10 and 20 N. The worn surfaces have been characterised using optical microscopy, scanning electron microscopy, energy dispersive X-ray spectroscopy and microhardness measurements. Plastic deformation and ploughing have been observed on the worn surfaces. The stresses imposed by friction near the surface caused a slight deformation of lamellae followed by interlamellar boundaries slip resulting in the inter-lamellar cleavage and subsequently their fracture. Micro-fracture from the inter-lamellar cracks resulted in the separation of fine-grained and flake-like debris. © 2000 Elsevier Science S.A. All rights reserved.

Keywords: Sliding wear; Titanium aluminides

1. Introduction

Gamma-based titanium aluminides have been developed for high temperature applications such as required by the aerospace industry [1,2]. These materials have been recently recognised to have wider application [3–5], for example as a material for use in automotive exhaust valves, utilising their high strength-to-weight ratio, high strength at elevated temperatures and the corrosion and oxidation resistance of the material. The major obstructions to the use of these materials in the past have been poor toughness and elongation at room temperature. Considerable effort in the last 10 years has improved these properties enough for more application-specific properties to grow in importance, one such property being tribological behaviour.

There is a limited information concerning the mechanisms involved in the sliding wear behaviour of gamma-based titanium aluminides [6]. A preliminary study [7] on the hardness and wear properties of these alloys has shown them to have a low hardness and poor wear, comparable with conventional titanium alloys. However, the metallurgy of these materials differs significantly from that of

conventional titanium alloys and some basic understanding of the tribological behaviour of gamma titanium aluminides needs to be established. It is also likely that some form of surface engineering for protection against wear damage may be necessary to exploit this type of material [8–10], and therefore, some prior knowledge of the wear behaviour of the substrate material is necessary.

This paper describes the results of dry sliding wear of lamellar Ti–48Al–2Nb–2Mn and Ti–45Al–2Nb–2Mn–1B alloys carried out against bearing steel. The characteristics of the worn surfaces and the operating wear mechanisms are discussed.

2. Experimental work

The Ti–48Al–2Nb–2Mn and Ti–45Al–2Nb–2Mn–1B titanium aluminides were manufactured using a twin torch Retech plasma furnace. Elemental compacts were semi-continuously cast into 100-mm-diameter ingot. The as-cast alloys were sectioned by Electrical Discharge Machining (EDM) to circular discs for wear testing which were then ground to a surface finish of between 0.02 and 0.4 μm (Ra). The surfaces were cleaned with acetone to remove contaminants before wear tests.

Sliding wear tests were conducted under atmospheric conditions using a ball-on-disc wear test system, which is

* Corresponding author. Tel.: +44-121-414-5245; fax: +44-121-414-5232.

E-mail address: a.r.rastkar@bham.ac.uk (A.R. Rastkar).

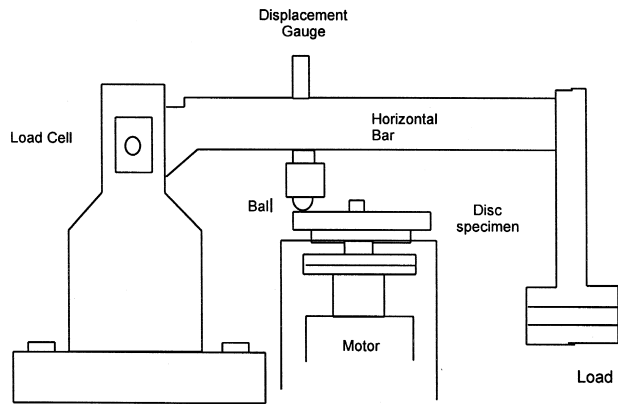


Fig. 1. Schematic diagram showing the ball-on-disk wear configuration.

shown in Fig. 1. Bearing steel balls (52100) of 10-mm diameter, and 720 HV_{0.5} hardness were run against horizontal rotating titanium aluminides discs with the hardness of 320–420 HV_{0.5}. The disc was driven by a servo-controlled DC motor, capable of providing a continuously variable range of rotating speeds. Loads were applied to

the ball through a load arm by means of a flat spring, designed to reduce inertial loading. Experimental friction data were collected and displayed graphically using a personal computer connected via an analogue-digital converter to a strain gauge. The applied loads were 5, 10 and 20 N which correspond to the maximum Hertzian normal contact stresses [11] of 746, 940 and 1184 MPa, respectively between ball and disc. The relative speed of the disc and rider was 100 mm s⁻¹.

Volume wear loss was measured by calculating the worn volume of the wear track on the surface. This measurement was carried out through a profilometer moving across the wear track width. The worn surfaces were studied using optical microscope and scanning electron microscope, having the facility for energy dispersive X-ray spectrometry (EDS). Fracture sections through worn material were examined using high resolution SEM (FESEM). The specimens were prepared by fracturing the samples across the surface layers to be studied using a notch in the back face of the worn surface to initiate the fracture. In fact the fractured surfaces are either from the bulk of the

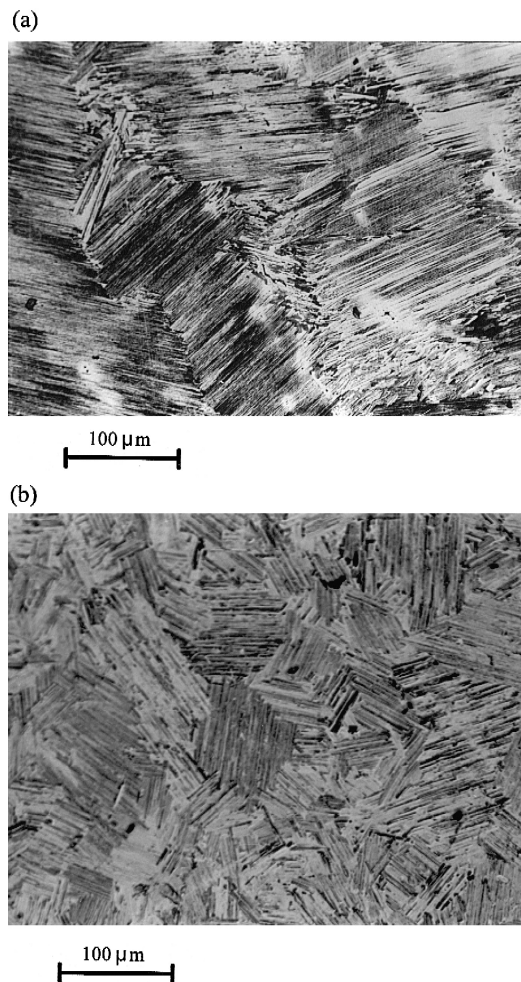


Fig. 2. Optical micrographs of the lamellar structure of (a) Ti-48Al-2Nb-2Mn and (b) Ti-45Al-2Nb-2Mn-1B alloys.

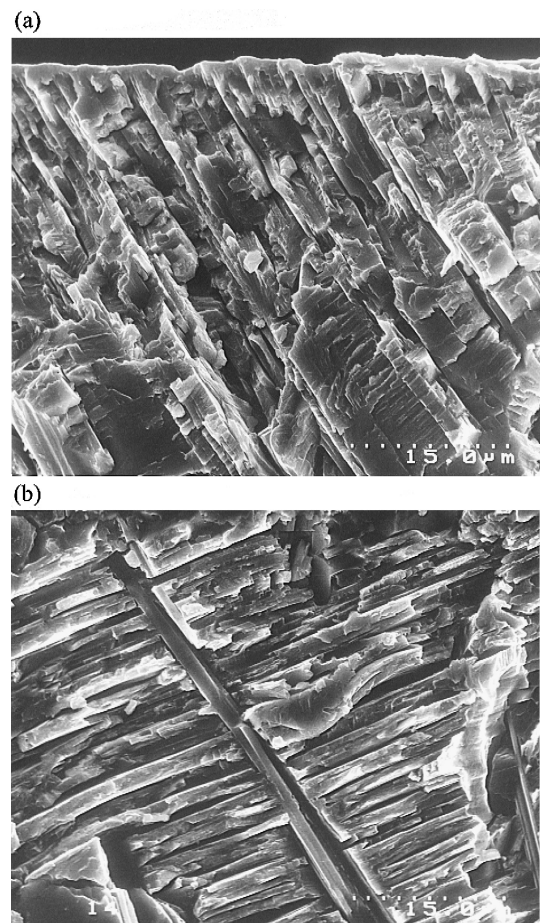


Fig. 3. FESEM micrographs showing the fracture cross-section of lamellar structure of (a) Ti-48Al-2Nb-2Mn and (b) Ti-45Al-2Nb-2Mn-1B alloys.

material to show the lamellar structure or perpendicular to the worn surface to show the lamellae deformation.

3. Results

3.1. Microstructure characterisation

The microstructure of Ti-48Al-2Nb-2Mn and Ti-45Al-2Nb-2Mn-1B alloys is shown in Fig. 2. Ti-48Al-2Nb-2Mn alloy (Fig. 2a) is composed of coarse columnar grains about 500 μm whereas Ti-45Al-2Nb-2Mn-1B alloy (Fig. 2b) is fine grained between 50 and 100 μm , due to Boron addition which forms TiB_2 needle or plate-like particles within the grains. Nevertheless, the alloys had quite different grain size, the lamellae size of the alloys was not very different. This can be seen in Fig. 3, which shows the fracture cross-section of these alloys. It can be seen in Fig. 3b that the TiB_2 plate has interrupted the pattern of lamellar structure in the surrounding matrix.

3.2. Material loss

The material loss for Ti-48Al-2Nb-2Mn and Ti-45Al-2Nb-2Mn-1B alloys increases proportionally with sliding distance at all applied loads (Fig. 4). For Ti-48Al-

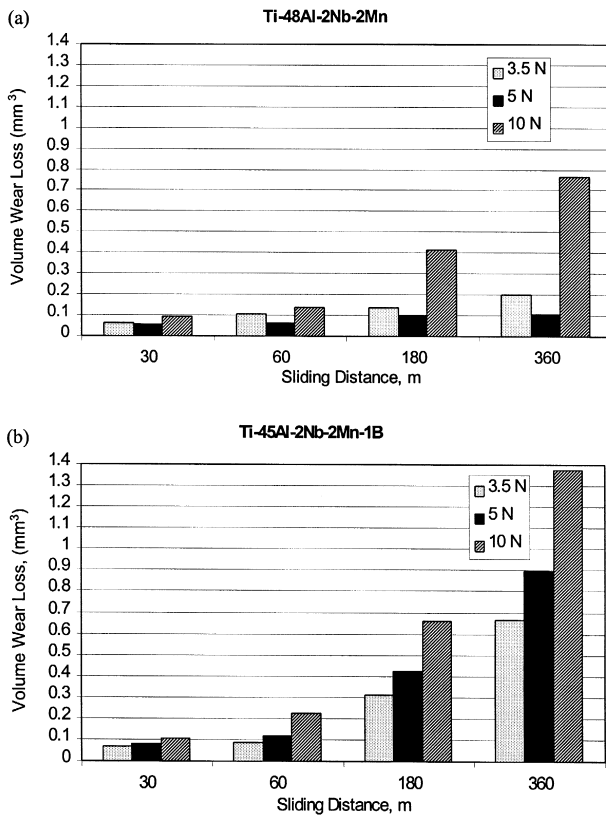


Fig. 4. Volume loss against sliding distance for lamellar structures of (a) Ti-48Al-2Nb-2Mn highlighting its anomalous behaviour at 5-N load and (b) Ti-45Al-2Nb-2Mn-1B alloys.

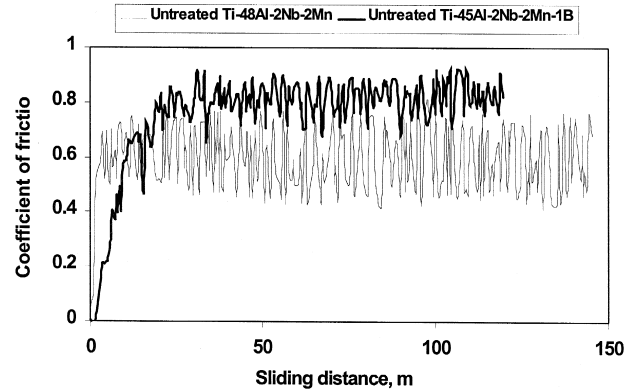


Fig. 5. Typical friction curves obtained for fully lamellar structures of (a) Ti-48Al-2Nb-2Mn and (b) Ti-45Al-2Nb-2Mn-1B alloys under 5-N load and 0.1 m/s.

2Nb-2Mn sample, Fig. 4a, at the lower loads of 3.5 and 5 N, after an initial running-in period, there is a much lower

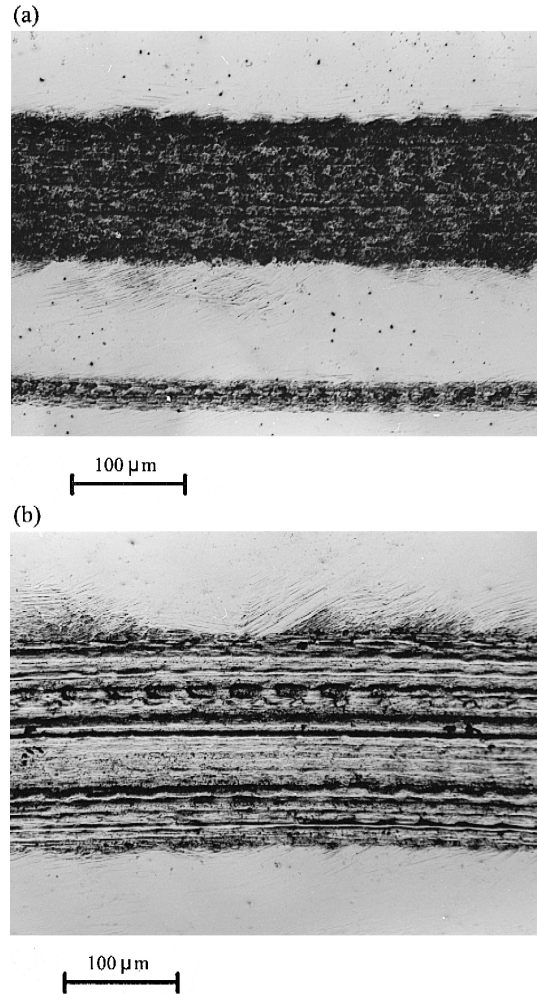


Fig. 6. Optical micrographs showing the plastic deformation and ploughing of the wear tracks produced on Ti-48Al-2Nb-2Mn alloy under (a) 5 N load having more oxide products on the surface and (b) 10-N load with less oxides.

increase in material loss with sliding distance if compared to 10 N load. In the case of Ti–45Al–2Nb–2Mn–1B alloy, Fig. 4b, the wear rates, represented indirectly by plots of volume loss against sliding distance, are approximately constant throughout the duration of the test. For all three loading conditions, the wear measured for Ti–45Al–2Nb–2Mn–1B alloy was greater than that for Ti–48Al–2Nb–2Mn alloy in equivalent tests.

With regard to the load effect in material loss, a relatively low amount of material loss was observed for Ti–48Al–2Nb–2Mn alloy (Fig. 4a) at 5 N applied load, or in fact this alloy had an anomalous behaviour at 5 N load, while for that of Ti–45Al–2Nb–2Mn–1B alloy (Fig. 4b), it was nearly proportional to the load increase.

3.3. Friction

Under all loads the friction tests on Ti–48Al–2Nb–2Mn and Ti–45Al–2Nb–2Mn–1B alloys showed scattered varying coefficient of friction. Typical friction traces of these alloys are shown in Fig. 5. All the coefficients of friction measured fell within the range of 0.5–0.8.

3.4. Worn surfaces

Under all loads, uneven surfaces were produced by plastic deformation and ploughing. Fig. 6a and b show this feature on the worn surfaces of Ti–48Al–2Nb–2Mn alloy

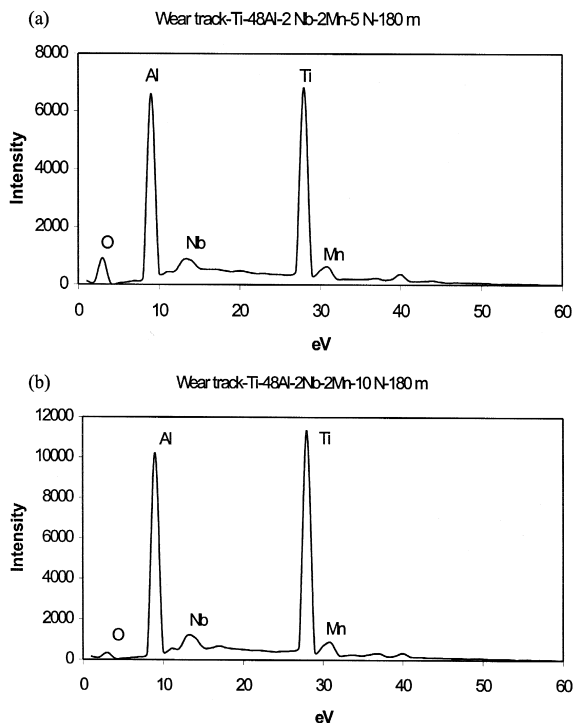


Fig. 7. EDS patterns show the level of oxygen combined with the worn surfaces of Ti–48Al–2Nb–2Mn after wear test under (a) 5 N and (b) 10-N load.

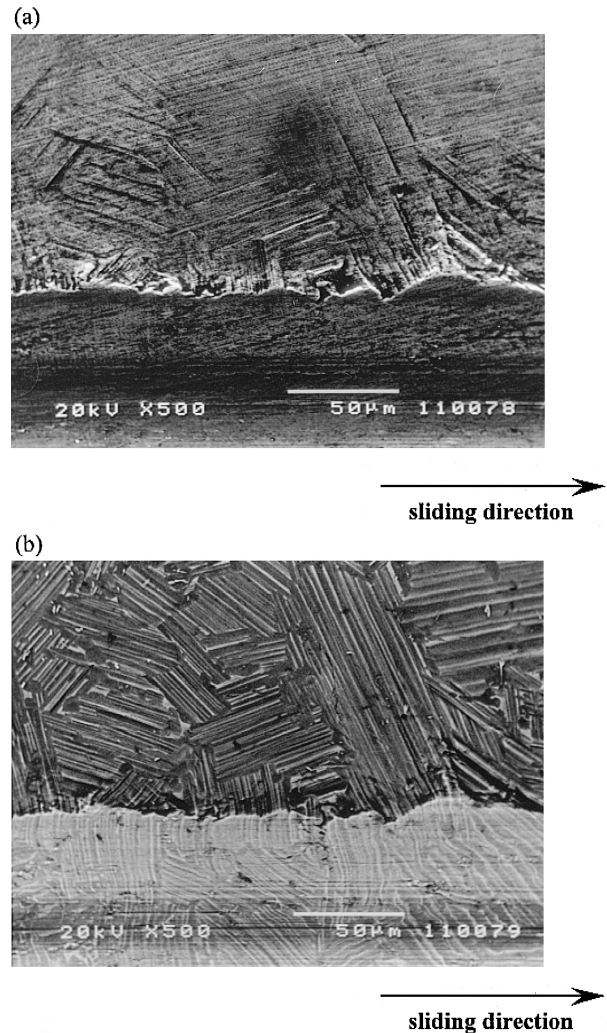


Fig. 8. SEM micrographs showing the extruded step like pattern adjacent to the wear track of Ti–45Al–2Nb–2Mn–1B alloy produced under 20-N load, (a) secondary electron image and (b) backscattered electron image.

after wear tests under 5 and 10 N, respectively. The wear track produced under 5 N (Fig. 6a) had a darker colour than that of 10 N load. EDS analysis (Fig. 7a and b) from wear tracks showed a higher oxygen on that of 5-N load.

3.5. Areas adjacent to the wear tracks

After all the wear tests, some surface markings adjacent to the wear tracks in the unworn area were noted. SEM imaging of the wear tracks produced at high load tests revealed that these patterns originate from the lamellar microstructures of the materials or in fact they are extruded step-like (ESL) lines originating from the lamellar pattern. The secondary electron micrograph in Fig. 8a shows the ESL pattern adjacent to a wear track on a polished Ti–45Al–2Nb–2Mn–1B sample produced after the 20 N applied load test, indicating some surface relief. The degree of ESL pattern lessens away from the wear

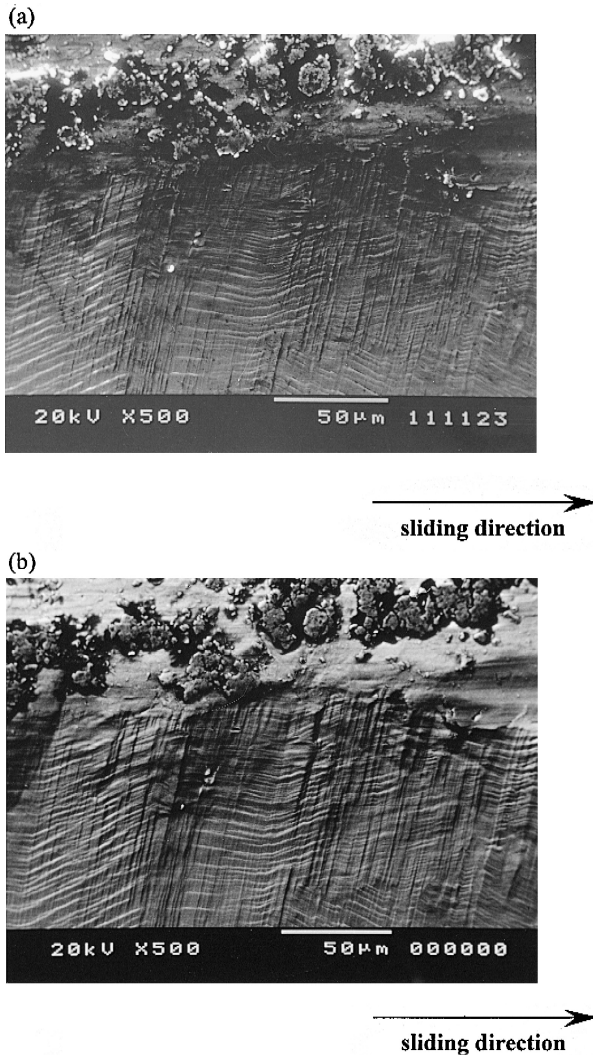


Fig. 9. SEM micrographs showing the extruded step-like pattern adjacent to the wear track on Ti-48Al-2Nb-2Mn alloy associated with crossed slip lines across the lamellae at 20-N load. (a) Secondary electron image, (b) Backscattered electron image.

track. Fig. 8b is a back-scattered electron micrograph of the same area, in which the contrast is produced from the compositional difference between the adjacent lamellae of TiAl and Ti₃Al. It can be seen that the marking observed in the secondary electron image corresponds to the microstructure shown in the back scattered electron image.

A comparison of these two figures shows the relationship between the surface relief and the microstructure. The effect is much clear in this alloy because of its fine grain size and slightly thicker lamellae. It can clearly be seen that a group of parallel lines in relief (Fig. 8a) correspond to an individual grain (Fig. 8b). These lines from Fig. 6b can be seen to continue, with some slight disruption, into the wear track. The slip lines appeared more or less across the lamellae, which were more visible in the lamellae extending approximately perpendicular to the wear tracks in the coarse grained Ti-48Al-2Nb-2Mn. Fig. 9a and b

shows the secondary electron and back-scattered electron images of these lamellae, which can be superimposed and compared in the same way as in the previous section. The slip lines and possibly microtwins are nearly perpendicular to the lamellae [12].

3.6. Deformation of lamellae

Etching of the worn and deformed surfaces revealed clearly some interlamellar cracks (Fig. 10) extending into the unworn areas adjacent to the wear tracks. The cracks were more visible after etching since a highly deformed, thin layer covering some cracks was removed from the surface.

Longitudinal fracture cross-sections through wear tracks revealed the extent of deformation of the lamellar structure beneath the wear tracks. Fig. 11 show the slight deformation or bending of lamellae and interlamellar boundary slip in worn surface (Fig. 11a) and the area adjacent to the wear tracks (Fig. 11b) of Ti-48Al-2Nb-2Mn alloy. The cross slip lines can be also observed in the area adjacent to the wear tracks (Fig. 11b). From Fig. 12 it appears that some transgranular fracture has occurred across the lamellae in Ti-45Al-2Nb-2Mn-1B alloy at the point of bending (at approximately 10 μm depth) in addition to the intergranular cracks.

3.7. Wear debris

The wear debris of these lamellar intermetallic alloys were in a wide range. Fig. 13 shows the debris of Ti-48Al-2Nb-2Mn and Ti-45Al-2Nb-2Mn-1B alloys produced after the 10 N applied load tests. The debris of Ti-48Al-2Nb-2Mn alloy is a mixture of rounded edge and mostly plate like particles and the debris of Ti-45Al-

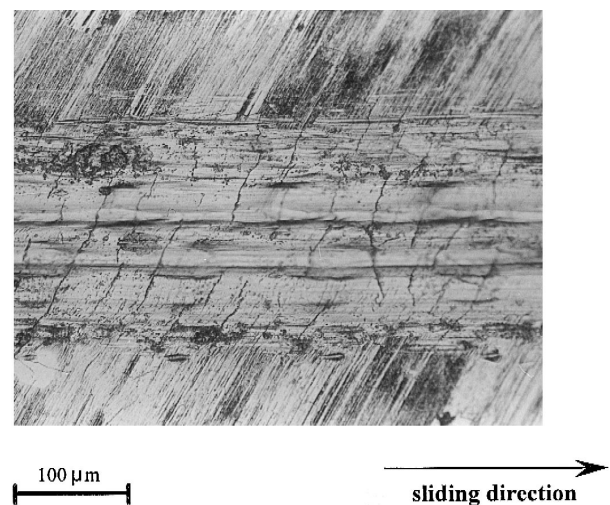


Fig. 10. Optical micrograph showing the cracks resulted from plastic deformation and ploughing of the wear track produced on Ti-48Al-2Nb-2Mn titanium aluminide at 10-N load.

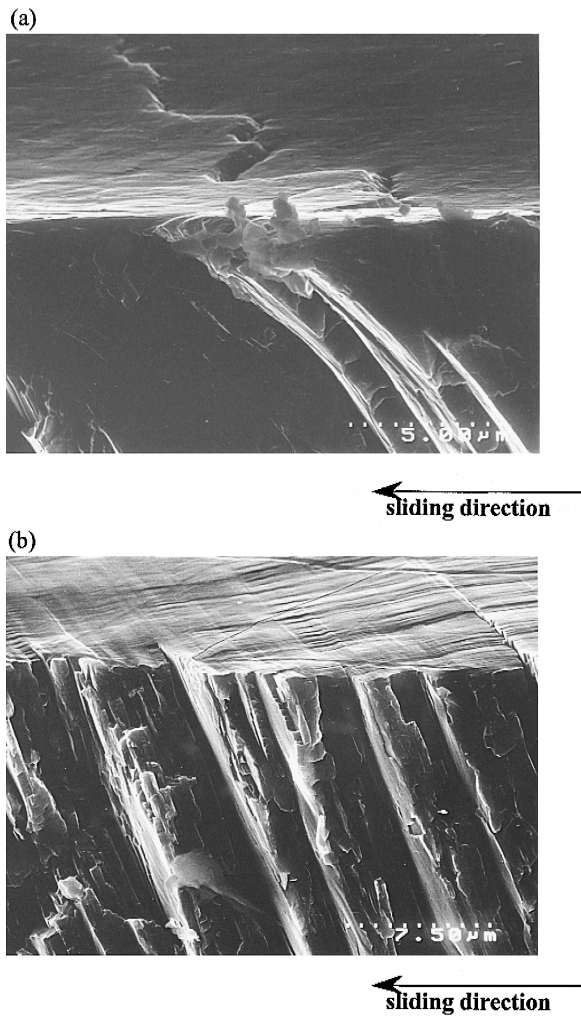


Fig. 11. FESEM micrographs of worn Ti-48Al-2Nb-2Mn alloy showing a slight deformation of lamellae and interlamellar boundary slip at 20-N load in (a) the wear track and (b) the extension interlamellar boundary slip and associated cross slips into the area adjacent to the wear track.

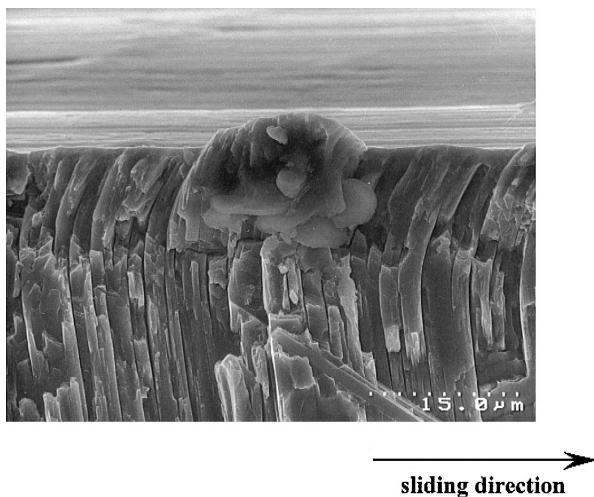


Fig. 12. FESEM micrograph showing the deformation of Ti-45Al-2Nb-2Mn-1B lamellae and their fracture at the point of bending at 20-N load.

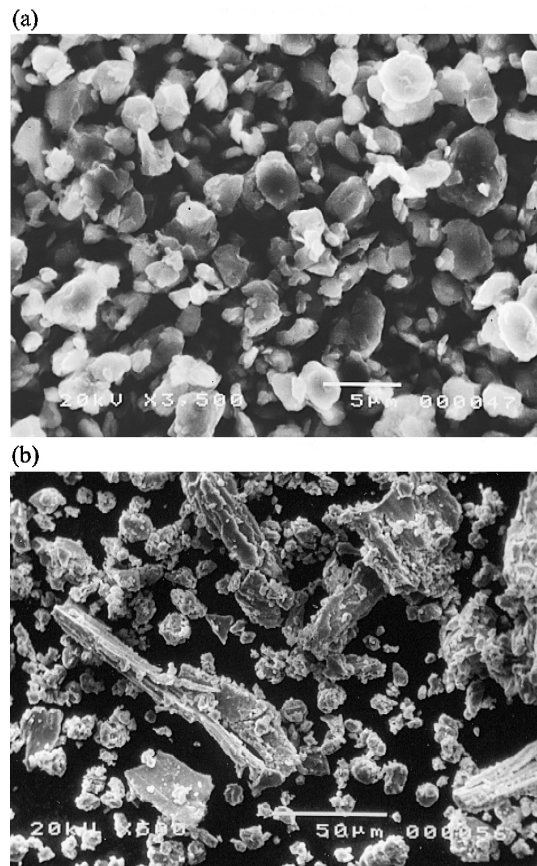


Fig. 13. SEM micrographs showing the morphology of the debris obtained from (a) Ti-48Al-2Nb-2Mn and (b) Ti-45Al-2Nb-2Mn-1B alloys at 10-N load.

2Nb-2Mn-1B alloy is a mixture of fine and coarse irregular particles with predominating plate-like debris.

4. Discussion

It may be stated that unlike the grain refinement, the Boron addition has had a negligible effect on the lamellae size of the Ti-45Al-2Nb-2Mn-1B alloy. Moreover as can be seen in Fig. 3b that the TiB_2 plate interrupts the pattern of lamellar structure in the surrounding matrix. This notch shaped interruption may be considered as a suitable place for crack initiation in Ti-45Al-2Nb-2Mn-1B alloy during sliding wear.

According to Hertz's analysis [11] if a sphere of an elastic material pressed against a plane, the maximum shear stress under the surface is 0.47 times of mean pressure on the surface. However, in this analysis the surface is considered smooth and without friction, where as in real rough contact surfaces the stress level is three times higher [13]. Under normal loads of 5, 10 and 20 N, the mean normal contact pressures according to Hertz's analysis were calculated as 497, 627 and 790 MPa which were beyond the yield strength and consequently the shear

Table 1

Properties of gamma-based titanium aluminides

Y.W. Kim, F.H. Froes, High Temperature Aluminides and Intermetallics, in: S.H. Whang, C.T. Liu, D. (Eds.) 112 Minerals, Metals and Materials society, 1990, pp. 465–492.

Structure	L1 ₀
Density, g/cm ³	3.7–3.9
Modulus, GPa	160–180
Yield Strength, MPa	400–650
Tensile Strength, MPa	450–800
Ductility, % at RT	1–4
Ductility, % at HT	10–60
Fracture Toughness, MPa m ^{-1/2}	10–20

strength of TiAl-based alloys (Table 1). Therefore, the applied loads could cause slip (Figs. 8 and 9) and cracks (Fig. 10) in the inter-lamellar boundaries. The cross-slip creates the slip lines or steps, which are perpendicular to the interlamellar boundaries (Fig. 10). It has been proposed and shown that fracture in lamellar microstructures is more likely to be initiated from these locations [12]. Moreover, the highly stick-slip friction behaviour of titanium aluminides which is a characteristic of these materials results in a high stress, which causes the slight deformation or bending of lamellae and subsequently the interlamellar slip, cross slip and consequently the cleavage of interlamellar boundaries. It is clear from Figs. 11 and 12 that this interlamellar fracture occurs in the wear tests.

The high stress levels resulting from friction cause dislocation activity in the volume of material adjacent to the wear track. Evidence for this are the lamellae bending (Fig. 12) and the extension of interlamellar boundaries slip (Fig. 9) into the area adjacent to the wear tracks. The degree of deformation exhibited by the lamellae is very large for this brittle material. In other low toughness materials such as minerals, the high hydrostatic pressures developed around scratch and indentation tests have suppressed brittle failure [14] and non-brittle behaviour has been observed in ceramic subjected to abrasion [15]. Scratch tests have recently been shown to produce significant plastic deformation in columnar TiN [16].

The general appearance of the wear tracks was composed of plastic deformation and ploughing. The lack of any normal features of adhesive or abrasive wear, together with the nature of the debris, suggest that a micro-fracture mechanism be in operation. The interlamellar cracks in the wear track (Fig. 10), micro fracture evident on the surface, an example of which is the centre of Fig. 11a, and fine debris of both Ti–48Al–2Nb–2Mn and Ti–45Al–2Nb–2Mn–1B alloys, Fig. 12, indicate that material loss occurs at these cracks.

The phenomena of the low wear rate (Fig. 4a) and the anomalous behaviour of Ti–48Al–2Nb–2Mn alloy associated with the appearance of wear track of this sample under 5 N test (Fig. 6a) were further investigated. EDS examination on the wear tracks (Fig. 7) showed a signifi-

cantly larger oxygen peak corresponding to the 5-N wear test if compared to that of the 10-N test, implying more oxygen was produced on the worn surface under 5-N load. The oxygen is likely corresponded to TiO₂ oxide, which its lubricious nature reduces the wear and consequently wear loss. Therefore, it is thought that a relatively low and oxidative wear mechanism was in operation on Ti–48Al–2Nb–2Mn alloy where as a metallic wear occurred on Ti–45Al–2Nb–2Mn–1B alloy, which produced shiny worn surfaces on the material.

Examination of the wear debris from both materials showed the presence of flat plates of different sizes. The debris from the B containing alloy contained much larger pieces (Fig. 13b). The reasons for the different morphology of the debris between the two alloys are not clearly known. It may be suggested that the notch shaped interruption of lamellae by TiB₂ plate like particles was a suitable place for crack initiation and quick propagation and subsequent fracture of Ti–45Al–2Nb–2Mn–1B alloy in addition to the fracture mechanism explained above. The large and sharp edge particles of Ti–45Al–2Nb–2Mn–1B wear debris may be evidence of larger fracture and material removal in this alloy. Moreover, the sharp edge particles of Ti–45Al–2Nb–2Mn–1B wear debris may agglomerate and adhere to each other during sliding. The fine and rounded edge flakes of Ti–48Al–2Nb–2Mn debris have resulted more likely from oxidative wear behaviour of the alloy. The oxidation has removed the sharp edges and prevented from any further agglomeration and adhesion due to the lubricious nature of TiO₂ oxides produced during sliding.

5. Conclusions

The friction behaviour of Ti–48Al–2Nb–2Mn and Ti–45Al–2Nb–2Mn–1B titanium aluminides during sliding is highly fluctuating from 0.5 up to 0.8. Sliding of bearing steel causes a slight deformation of lamellae and slip through the interlamellar boundaries. Under this sliding conditions the interlamellar slip results in the cleavage and consequently fracture of lamellae in the worn area and the area adjacent to the wear tracks. Fractured lamellae may be agglomerated into large particles or fragmented under the subsequent abrasion action between the slider and worn surface into some fine and irregular wear debris in both alloys.

References

- [1] Y.W. Kim, D.M. Dimiduk, Progress in the understanding of gamma titanium aluminides, JOM 43 (8) (1991) 40–47, August.
- [2] Y.W. Kim, Microstructure/property relationships in titanium aluminides and alloys, in: Y.W. Kim, R.R. Boyer (Eds.), The Minerals, Metals & Materials Society, 1991, pp. 91–103.

- [3] S. Hurta, H. Clemens, G. Frommeyer, H.P. Nicolai, H. Sibian, Titanium' 95: Science and Technology, in: Proceedings of the Eighth World Conference on Titanium, 1995, pp. 97–104.
- [4] P.E. Jones, W.J. Porter III, M.M. Keller, D. Eylon, Mat. Res. Soc. Symp. Proc. 364 (1995) 769–774.
- [5] T. Noda, Intermetallics 6 (1998) 709–713.
- [6] C.L. Chu, S.K. Wu, Scr. Metall. Mater. 33 (1) (1995) 139–143.
- [7] A. Bloyce, (1994), Environmental Sensitivity of Surface Engineered Titanium Aluminides, EssenTiAl University Network, Meeting report.
- [8] A.R. Rastkar, M. Phil. Thesis, The University of Birmingham, 1997.
- [9] A.R. Rastkar, A. Bloyce, T. Bell, in: Second International Symposium on Intermetallics, Pittsburgh, USA, 21–23 Sept., 1997.
- [10] Y. Umakoshi, H.Y. Yasuda, T. Nakano, Intermetallics 4 (1996) s65–s75.
- [11] I.M. Hutchings Tribology: Friction and Wear of Engineering Materials, Edward Arnold, London, 1992, pp. 4, 46, 47.
- [12] Y. Umakoshi, H.Y. Yasuda, T. Nakano, Plastic Anisotropy and Fatigue of TiAl PST crystals: a review, Intermetallics 4 (1996) S65–S75.
- [13] K. Mao, Y. Sun, T. Bell, Contact mechanics of engineering surfaces: state of the art, Surf. Eng. 10 (4) (1994) 297–306.
- [14] D. Tabor, Br. J. Appl. Phys. 7 (1956) 159.
- [15] B.J. Hockey, J. Am. Ceram. Soc 54 (5) (1971) 223.
- [16] K.J. Ma, A. Bloyce, Surf. Eng. 11 (1) (1995) 71.